



NUMERICAL STUDIES OF FLOW FIELD
INSIDE ENCLOSURES

H.E.S.FATH* and M.M.SOROUR**

ABSTRACT

This paper study the transient and steady state two dimensional flow patterns inside enclosures of different geometries . A computer code is developed which uses a modified version of the Marker And Cell (MAC) numerical technique. Although the computer code is general it was applied to three configurations, viz rectangular cavity, vee-groove, and semicircular enclosure. The results are presented by velocity vectors which identify low and high velocity regions as well as flow circulation.

* Assistant Professor ** Associate Professor, Member of ASME
Mechanical Engineering Dept., Faculty of Engineering, Alexandria
University, Alexandria, Egypt.

1. INTRODUCTION

Full scale experimental testing of complicated engineering geometries and components, for design purposes, is getting more and more expensive and often technically difficult. Consequently, theoretical studies and specifically transient and steady multidimensional computer codes is increasingly becoming more important. These codes are used to analyse the aerodynamics (and hydrodynamic) characteristics of components and passages of general configurations. For example, the assessment of dynamic effects of transient flow field, and the flow induced vibration on structures depends upon the detailed information of the transient and steady pressure and velocity fields. In addition, the knowledge of the location of low velocity and stagnant regions helps deciding possible local corrosion and other engineering problems.

The theoretical analyses of flow problems inside enclosures involves the solution of the governing equations (transient, multidimensional, non linear partial differential equations) of continuity and momentum. The problem becomes more complicated when the enclosure geometry is not uniform. In an attempt to resolve this complex problem, this presentation deals with finite difference scheme for the transient flow field in two dimensional enclosures of different configurations.

2. MATHEMATICAL FORMULATION

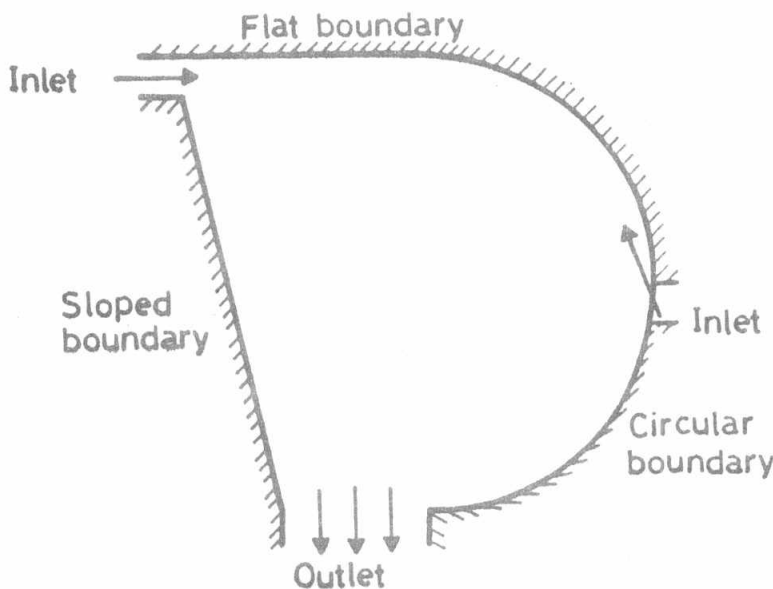


Fig.(1) General Enclosure Configuration.

Figure 1 illustrates an enclosure of different geometric boundaries, which will be termed a general configuration in this presentation. The mathematical formulation and code will apply to this general configuration while the computer runs will only be assessed for three specific geometries.

The dynamic characteristics of the fluid flow is governed by the conservation of mass and momentum equations. Therefore, for laminar, incompressible two dimensional flow these equations may be written as :

$$\text{Continuity Equation: } \frac{\partial u}{\partial x} + \frac{\partial v}{\partial y} = 0 \quad (1)$$

Momentum Equations

$$\frac{\partial u}{\partial t} + u \frac{\partial u}{\partial x} + v \frac{\partial u}{\partial y} = - \frac{\partial P}{\partial x} + \nu \left(\frac{\partial^2 u}{\partial x^2} + \frac{\partial^2 u}{\partial y^2} \right) \quad (2)$$

$$\frac{\partial v}{\partial t} + u \frac{\partial v}{\partial x} + v \frac{\partial v}{\partial y} = - \frac{\partial P}{\partial y} + \nu \left(\frac{\partial^2 v}{\partial x^2} + \frac{\partial^2 v}{\partial y^2} \right) \quad (3)$$

To solve the above equations (1) to (3) , the initial conditions and the appropriate boundary conditions must be specified. These conditions are written as follows.

i) Initial Conditions

The velocity components are assumed zero every-where inside the enclosure, although any other specified initial conditions may be used.

$$u(x,y,0) = v(x,y,0) = 0 \quad (4)$$

ii) Boundary Conditions

Top Boundary: For no-slip condition the fluid velocities at the wall are taken equal to zero ie

$$U(x, y_{\max}, t) = v(x, y_{\max}, t) = 0 \quad (5)$$

Bottom Boundary: The velocity component $v(x, y_{\min}, t)$ is adjusted to satisfy continuity equation, i.e.

$$u(x, y_{\min}, t) = \frac{\partial v}{\partial y} (x, y_{\min}, t) = 0 \quad (6)$$

Side Boundaries: no-slip condition at the wall

$$u(x,y,t) = v(x,y,t) = 0 \quad (7)$$

Therefore zero velocity component are applied every-where at the sides boundaries except at the location of inlet flow where the inlet velocities are specified.

3. NUMERICAL TECHNIQUE

The numerical technique used in the present study is based on the finite difference algorithm developed by Hirt⁽¹⁾ (see also reference (2)). In this technique the computation region is divided into a number of rectangular cells of width Δx and height Δy , figure 2. The fluid region is surrounded by a single layer of fictitious cells where the boundary conditions are to be specified. To distinguish between different types of cells the computation region is flagged ie fluid cells are given cells number 1 while other numbers are assigned to boundary cells. Therefore adequate velocity boundary conditions are imposed, see table 1.

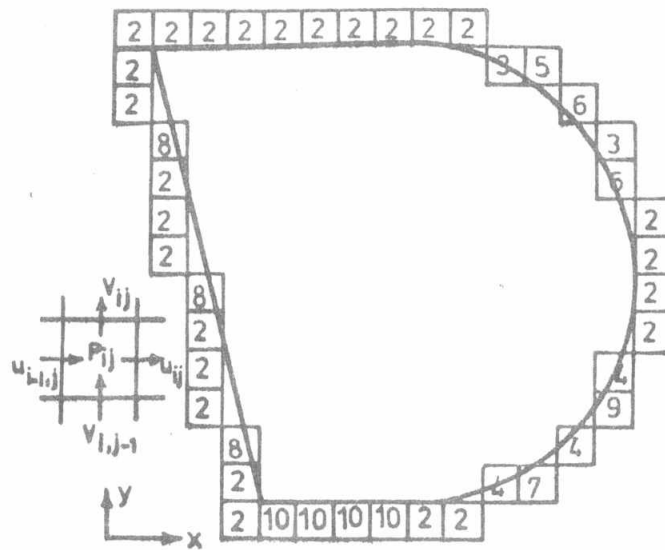


Fig.(2) Finite Difference Grid .

Table 1. Velocity boundary conditions

Cell No.	Boundary conditions
2-right	$U(I \text{ MAX}-1,J)=0$, $V(IMAX,J)=-v(IMAX-1,J)$
2-left	$U(I,J)=0$, $V(I,J)=-V(I+1,J)$
2-top	$U(I,JMAX)=-U(I,JMAX-1)$, $V(I,JMAX-1)=0$
2-bottom	$U(I,1)=-U(I,2)$, $V(I,1)= 0$
3	$U(I-1,J)=0$, $V(I,J-1) = 0$
4	$U(I-1,J)=0$, $V(I,J) = .0$
5	$U(I-1,J)=-U(I-1,J-1)$, $V(I,J-1)=0$
6	$U(I-1,J)=0$, $V(I,J-1)=-V(I-1,J-1)$
7	$U(I-1,J) = - U(I-1,J+1)$, $V(I,J) = 0$
8	$U(I,J) = 0$, $V(I,J) = 0$
9	$U(I-1,J)=0$, $V(I,J)=-V(I-1,J)$
10	$U(I,1) = -U(I,2)$

The fluid velocity components, U and V, are defined at the cell boundaries while the pressure is defined at the cell center. Figure 2 shows an arrangement of the finite difference variables for a typical cell. The conservation equations 1 to 3 are then written in finite difference form as follows:

Mass conservation Equation

$$D = \frac{1}{\Delta x} (U_{iJ}^{n+1} - U_{i-1,J}^{n+1}) + \frac{1}{\Delta y} (V_{iJ}^{n+1} - V_{i,J-1}^{n+1}) < \epsilon \quad (8)$$

ϵ is the accuracy of the solution and approaches zero

Momentum Equation

$$U_{i,J}^{n+1} = U_{i,J}^n + \Delta t \left[\frac{1}{\Delta x} (P_{i,J}^n - P_{i+1,J}^n) - FUX - FUY + VISX \right] \quad (9)$$

$$V_{i,j}^{n+1} = V_{i,j}^n + \Delta t \left[\frac{1}{\Delta y} (P_{i,J}^n - P_{i,J+1}^n) - FVX - FVY + VISY + g \right] \quad (10)$$

where $FVX = U \left(\frac{\partial V}{\partial x} \right)_{i,j}^n$

$$= \frac{1}{2\Delta x} (V_{i+1,J}^n - V_{i,J}^n) (U_{i,J}^n - |U_{i,J}^n|) + \frac{1}{2\Delta x} (V_{i,J}^n - V_{i-1,J}^n) (U_{i,j}^n + |U_{i,J}^n|)$$

Expressions for FUX, FUY, VISX, FVY and VISY are similarly obtained and are omitted.

For the sloped and curved boundaries, the boundary cells velocity components are specified in such a way that for no slip boundary conditions the zero velocity is imposed at the real boundary rather than the cells boundary. This is done using either linear or parabolic interpolation. For example, using linear interpolation, the boundary cell velocity component U_2 , see figure 3 is defined as

$$U_2 = - \left(\frac{\ell}{x - \ell} \right) u_1$$

which is equivalent to zero velocity component U_w at the real wall w .

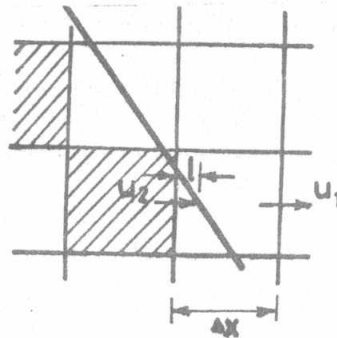


Fig.(3) Boundary Condition for sloped line.

To calculate the velocity and pressures the following steps are followed.

1. Compute estimates for the new velocity field from the momentum equations 9 and 10 .
2. Adjust the new velocity field iteratively to satisfy the mass conservation equation (8) by changing the cell pressures. If the divergence D of a cell in equation 8 is negative, this correspond to a net flow of mass into the cell, therefore the cell pressure must be increased to eliminate the net inflow. In addition, the pressure adjustment must be done iteratively since the adjustment of pressure in one cell affect adjacent cells. The pressure change required to make D equal to zero is

$$\Delta P = \frac{-D}{2 \Delta t \left[\frac{1}{(\Delta x)^2} + \frac{1}{(\Delta y)^2} \right]} \quad (11)$$

The new pressure, and velocity components after each iteration K are given by

$$P_{i,j}^{k+1} = P_{i,j}^k + \Delta P \quad (12)$$

$$U_{i,j}^{k+1} = U_{i,j}^k + \frac{\Delta t \Delta P}{\Delta x} \quad (13)$$

$$U_{i-1,j}^{k+1} = U_{i-1,j}^k - \frac{\Delta t \Delta P}{\Delta x} \quad (14)$$

$$V_{i,j}^{k+1} = V_{i,j}^k + \frac{\Delta t \Delta P}{\Delta y} \quad (15)$$

$$V_{i,j-1}^{k+1} = V_{i,j-1}^k - \frac{\Delta t \Delta P}{\Delta y} \quad (16)$$

3. When the new velocity field has been converged, the velocity and pressure fields are used as the starting values for the next time step cycle.

4. NUMERICAL STABILITY AND COMPUTATION TIME

Numerical stability is maintained provided the mass and momentums are not permitted to cross more than one cell at any time interval. Thus, the time increment must satisfy the usual Courant number criterion, for explicit schemes:

$$C_x = |U| \Delta t / \Delta x < 1.0 \quad C_y = |V| \Delta t / \Delta y < 1.0 \quad (17)$$

$$\text{and } \Delta t < \frac{1}{2v} \frac{(\Delta x)^2 (\Delta y)^2}{(\Delta x)^2 + (\Delta y)^2} \quad (18)$$

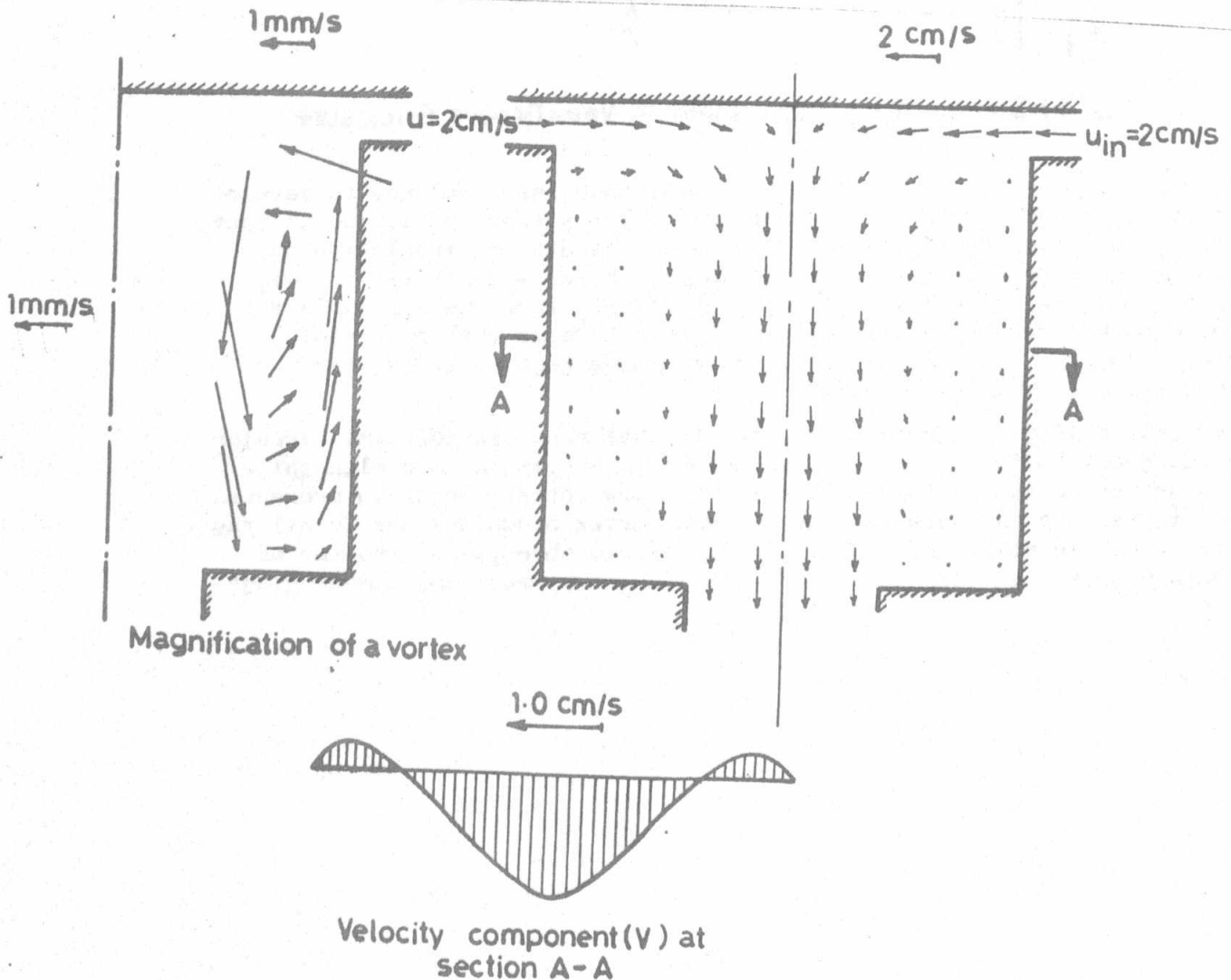
On the other hand, the computation time required per time increment depends in general on the following items. (1) The number of cells, (2) the cell size, (3) the time step and (4) the convergence criterion (ϵ) set for the velocity field iteration to satisfy the continuity equation (8). However the cell size and time step size are interrelated by the stability conditions. In addition, the number of cells depends upon the required detailed local information within the computation region and varies with the physical parameters of the problem.

Computational Results

Three different enclosures are studied to assess the capability of the present numerical code and to demonstrate the treatment of the

the boundary conditions. The first enclosure is a rectangular cavity which has two symmetric inlet sections and one common mid position outlet. ie symmetric flow patterns is expected with this configuration . It can be seen in figure 4, which illustrate the flow field in vector form, that symmetry is maintained and a mirror image is obtained around the vertical centerline. In addition, the velocity vector change its magnitude and direction significantly, especially near the side walls where large vortex is present. A magnified vector pattern for the vortex and a velocity profile at a mid horizontal plane is also illustrated in the same figure.

The complexity of the problem is increased by using sloped boundaries in the vee type enclosure. The assumed inlet and outlet locations is similar to that of the rectangular cavity and consequently due to symmetry only one half of the configuration is presented. Figure 5 illustrate the velocity vectors in two vee type enclosures with identical inlet velocities but different viscosity fluids, specifically air and highly viscous oil are compared.



Fig(4) Steady State Flow Field in Rectangular Enclosure

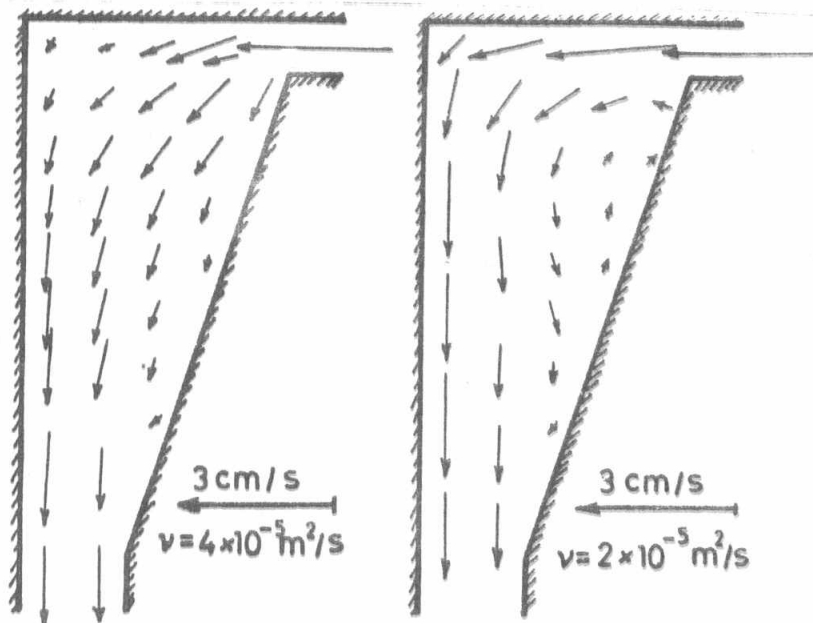


Fig.(5) Steady State Flow Field in Vee-Groove Enclosure

It can be seen that highly viscous fluids have less tendency to develop circulation and vortex motion compared to low viscosity fluids. In fact the velocity vectors for the former case indicate no circulation and nearly one directional flow. Furthermore, comparison between the Vee groove and the rectangular cavity case reveals that the vortex in the vee groove decrease in size and is shifted towards the upper region of the cavity. This feature indicate the advantage of the tilted boundaries in such flow conditions.

The last configuration to be studied in this paper is the semi-circular enclosure with inlet section just below the horizontal mid plan while the outlet at the enclosure bottom. The flow pattern which is presented in figure 6 is characterized by a large vortex occupying nearly all the enclosure. In addition, a small vortex is also observed at the top of the enclosure at which the velocities are very small and almost stagnant.

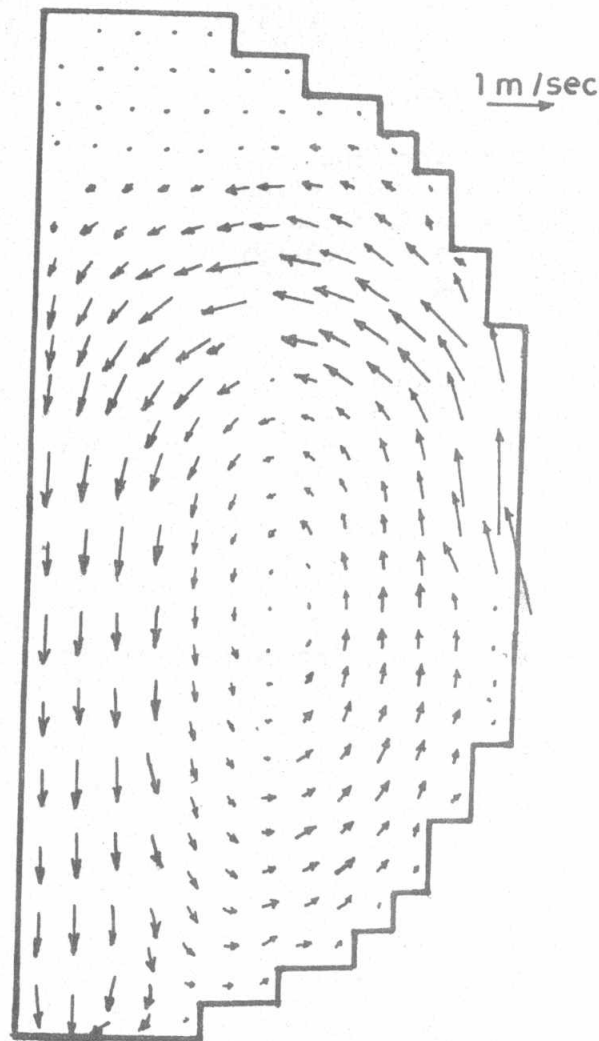


Fig.(6) Steady State Flow Pattern
Inside Half Circular Enclosure.

CONCLUSIONS

A numerical code has been developed to analyse the transient as well as the steady state two dimensional flow distributions inside general configuration enclosures. Three types of enclosures were presented, viz rectangular, vee-groove and cemicircular shape. The computational results were verified qualitatively against symmetry. The velocity vectors, vortices and stagnation areas were identified. The presented code was proved to be simple, flexible and can be extended to analyse the three dimensional problems.

REFERENCES

1. Hirt, C.W., Nichols, B.D, and Romero N.C" SOLA-A Numerical solution Algorithm for transient fluid flows" LA-4582, Jan 1975.
2. Roache. P.J " Computational fluid Dynamics" 1972.

NOMENCLATURE

D	Divergence Defined by Equation (8)	$m/s/m^2$
g	Gravitational Acceleration	m/s^2
i	Subscript Representing The Direction	
IMAX	Maximum Number of Cells along x-Direction	
j	Subscript Representing the y-Direction	
JMAX	Maximum Number of cells along y-Direction	
n	Superscript Representing Time	
P	Pressure/Density ratio	N.m/kg
t	Time	
u	Velocity component in x-direction	m/s
v	Velocity component in y-direction	m/s
x	Coordinate in x-direction	
y	Coordinate in y-direction	

Greek Letters

Δ	Incremental Step Size	
ν	Kinematic viscosity	m^2/s
ϵ	Small Number Representing Accuracy (of order of 10^{-4})	